Geologie en Mijnbouw 67: 363–378 (1988)

Geochemical variations in a Proterozoic hydrothermal mafic breccia dyke related to Ni-Cu-Fe skarn mineralization at Annehill, Bergslagen, Sweden

James H. Baker[1], Lars-Gunnar Andersson[2] & Andromachi Marinou[3]
[1] *Geological Museum, University of Amsterdam, Nieuwe Prinsengracht 130, 1018 VZ Amsterdam, The Netherlands; present address: Instituut voor Aardwetenschappen, Rijks Universiteit Utrecht, P.O. Box 80.021, 3508 TA Utrecht, The Netherlands;* [2] *SGAB Prospektering AB, Håksberg, 77100 Ludvika, Sweden;* [3] *Department of Geology, University of New Brunswick, Box 4400, Fredericton NB, Canada E2B 5A3*

Received 2 July 1987; accepted in revised form 26 December 1987

Key words: Breccia dyke, Ni-Cu-Fe skarn, hydrothermal alteration, geochemistry, Proterozoic, Sweden

Abstract

Nickel sulphide breccias form an uncommon type of Ni mineralization. The development of a Proterozoic mafic breccia dyke and Ni-Cu-Fe skarn in felsic metavolcanic wall rocks at Annehill, Bergslagen, Sweden, is genetically related to the emplacement of a continental tholeiite dyke. Hydrothermal alteration prior to and during brecciation distinguishes this mineralization from intramagmatic Ni mineralizations. Breccia development can be divided into two stages:

An initial pre-brecciation stage of pervasive alteration of the felsic metavolcanics produced minerals in the paragenetic order hydromuscovite-tourmaline-phlogopite-amphibole. Microprobe data shows this corresponds to B, F and Cl metasomatism respectively, and can be correlated with major element variations. High Ti mobility is demonstrated by the development of sphene poikiloblasts in the metavolcanics.

A second stage of mechanical fracturing developed a 1 km long, up to 20 m wide, breccia zone, with fragments of more or less altered metavolcanics in an amphibole matrix. Amphibole compositions become more Fe-rich closer to the tholeiitic dyke, which itself has undergone autometamorphism, with no magmatic minerals present.

Fe and V provide the best indicators of chemical variation in the altered rocks, breccia dyke and tholeiite. Highest B contents coincide with highest K, Rb, Li and Co in the altered rocks. There is a steady decrease in Fe, V, Ti, Mn, Co, and P from the tholeiite through the breccia and pervasively altered metavolcanic to least altered metavolcanic. With decreasing Fe there is an increase in Ca, Mg, and K, and Fe also shows a positive correlation with Be, Pb, Sc and Eu.

REE contents of pervasively altered and brecciated samples generally lie between those of the least altered metavolcanic and the tholeiitic dyke. This supports a model for contamination of the felsic metavolcanics with material derived from the tholeiite dyke.

The skarn ore comprises pyrrhotite with minor chalcopyrite and pyrite, and is located along the eastern margin of the breccia. Ni and V contents increase to 0.7%.

Emplacement of the tholeiitic dyke, along a pre-existing fracture, initiated a hydrothermal cell in the upper crust. Volatiles derived mainly from the wall rocks were responsible for the alteration of the felsic metavolcanics. At the same time a Ni-bearing hydrothermal phase developed in the crystallizing magma.

Brecciation could have been triggered by fault movements or pressure build up in the hydrothermal cell. Pressure release through brecciation allowed injection of the Ni-bearing hydrothermal phase into the felsic wall rocks to form the skarn mineralization along one side of the breccia dyke.

Introduction

Several minor Ni-Cu-Fe occurrences are known in the Bergslagen ore province of Central Sweden, including the mined out deposits of Kleva, Kuså, and Slätterberg (Nilsson, 1985).

While several magmatic Ni-mineralizations are known from the Baltic shield, there are few descriptions of breccia-related Ni-mineralizations in Scandinavia, mostly intramagmatic, including Skjaekardale, Norway (Boyd & Nixon, 1985). Hydrothermal breccia mineralizations are not recorded.

Ni occurrences in the area around Annehill (also known as Gåstjärn) are discussed by Blomberg (1879), Nilsson (1985) and Zakrzewski (1988). The area was previously investigated by the exploration companies SGAB and Boliden Mineral for Cu and W respectively. LKAB Prospektering recently carried out an assessment of the Pt potential of Ni-mineralization at Annehill. This paper is based partly on the results of that investigation, and discusses the setting, petrology and geochemistry of the hydrothermal mafic breccia dyke and mafic intrusive, and the skarn alteration process which was responsible for the minor Ni-Cu-Fe mineralization developed along one edge of the breccia dyke at Annehill.

Geological relationships

Western Bergslagen comprises a thick felsic sequence of metavolcanics and metasediments, the 1.9–1.86 Ga Bergslagen Supracrustal Sequence, now recognised as a manifestation of an aborted mid-Proterozoic submarine continental rifting event (Oen et al., 1982; Oen 1987). Mafic magmatism is restricted to a single short period of bimodal igneous activity at the close of felsic volcanism. Granites of a 1.9–1.86 Ga and a 1.8–1.78 Ga generation are recognised. An age of 1.84 Ga has been determined for the peak of regional metamorphism (Moorman et al., 1982). A post-rift, slightly younger age is assumed for W-Mo-Au mineralization (Baker & Hellingwerf, in press). The mafic breccia dyke crosscuts the felsic metavolcanics and is affected by a later phase of deformation, constraining the age of the breccia to between 1.9 and 1.84 Ga.

Geology of the area around Annehill

The area around Annehill comprises subvertical, NW-SE striking felsic metavolcanics of the 1.9–1.86 Ga Bergslagen Supracrustal Sequence (Fig. 1). In the western part of the area the rocks retain their pyroclastic character with relict high temperature quartz and feldspar phenocrysts and a fine grained quartz-feldspar matrix. Albitization and iron loss results in a white colouration in the rocks, but primary textures remain intact. In the eastern part of the area the effects of sub-seafloor hydrothermal alteration are apparent with the development of white coloured, quartz-Mg-chlorite-sericite schists, the original feldspar phenocrysts altering first to kaolin (see analyses, Baker & De Groot, 1983) and then Mg-chlorite. Relict fragments of felsic metavolcanics up to 25 cm are contained in the Mg schists to the west of the marble horizon (Fig. 1). A 3 m wide limestone horizon present within these schists has apparently escaped alteration with only minor tremolite and a few pyrrhotite and pyrite grains developed in a 10 cm wide zone along the contact with the schists. Mafic dykes run sub-parallel to the strike of the felsic rocks.

Several minor iron occurrences are present in the area. A magnetite skarn mineralization is located in the western part of the area (Fig. 1). All other mineralization is predominantly pyrrhotite with minor pyrite, chalcopyrite and occasional galena, and are thought to be related to the mafic breccia dyke. This predominance of Fe-sulphides contrasts

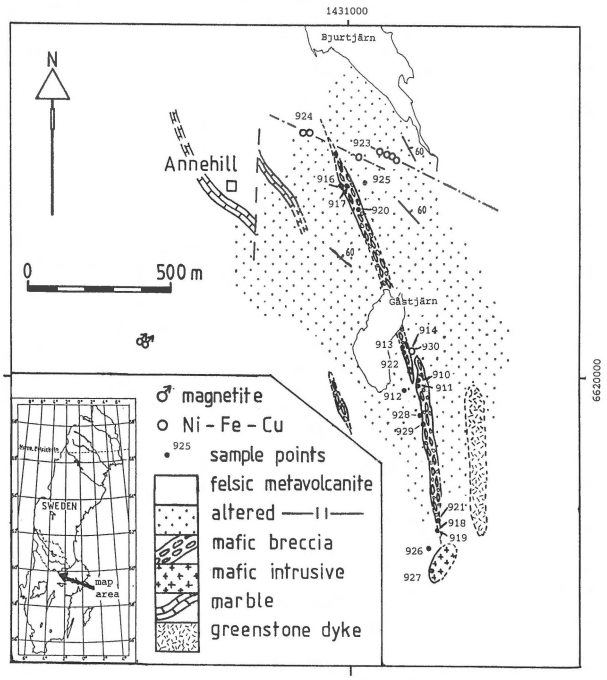

Fig. 1. Geological sketch map of the Annehill area, showing position of mafic breccia and Ni mineralizations. Swedish national grid coordinates shown.

with the Fe-oxide mineralizations which are generally present in this part of Bergslagen (Geijer & Magnusson, 1944). The mines at Gåstjärn lie along an approximately E-W trending fault, and contain ball ore, with pyrite, quartz and calcite 'balls', 2–5 cm, cemented in a matrix of pyrrhotite. Quartz veining with chalcopyrite is also abundant. Similar ball ore is present at the Yxsjön mine, south of the map area. A post-deformational minor phase of W-Mo mineralization is related to E-W quartz veins, skarn alteration and scheelite development occurring where Ca was available in the wall rocks.

Field, macroscopic and microscopic observations

The mafic breccia dyke

The mafic breccia dyke is a discontinuous development over 1 km, up to a few metres thick, and in some places fading out (Fig. 1), with angular fragments of felsic metavolcanite, from a few mm to cm in size, in an amphibole matrix. The felsic metavolcanic which is caught up in the breccia is almost always a hard, fine grained rock, differing from the Mg-chlorite-sericite schist which is the typical bedrock in this area, suggesting that pre-brecciation alteration may have occurred. In some blocks felsic metavolcanics can be seen to develop a network of lobate, 5 mm wide zones or patches of sericitic incipient alteration. In a later stage the sericitic patches are replaced by aggregates of green phyllosilicates. The intervening, more resistant, quartz-feldspar areas are apparently not affected by this alteration so that a spotted appearance is developed (Fig. 2a). This first stage pervasive alteration process, seen both in fragments in the breccia and surrounding wall rocks, is not accompanied by any brecciation.

In thin section the least altered felsic metavolcanic rock is seen to be an albitized crystal tuff, with relict magmatic quartz and feldspar grains. With the onset of alteration, irregular lobate aggregates of fine grained sericite up to 5 mm wide develop, which contain scattered stubby grains of light green tourmaline (Fig. 2b). The fine grained quartz-feldspar matrix of the felsic metavolcanics adjacent to the sericitic aggregates recrystallizes to a slightly coarser grained polygonal aggregate of quartz and K-feldspar. With progressive alteration the sericite aggregates become larger, while tourmaline growth increases to form large, single grains, or in some cases concentric overgrowths around the sericite. These tourmaline rims are in turn overgrown by rims of green-brown phlogopite (Fig. 2c), while phlogopite also replaces the sericite, and forms individual flakes in the matrix. This is responsible for the green spotting seen in the rock (Fig. 2a). The grain size of the matrix in the felsic metavolcanic also increases.

The second stage in the development of the breccia dyke is the brittle fracturing and brecciation, developed along the 1 km long zone shown in Fig. 1. Brecciation produced angular fragments of felsic metavolcanic rock from a few cm to 25 cm, showing various stages of incipient, pervasive alteration, in a matrix of almost pure amphibole (Fig. 2d). No great displacement or rotation of fragments could be seen in the breccia. The matrix takes the form of thin coatings between fragments, or may be up to


A

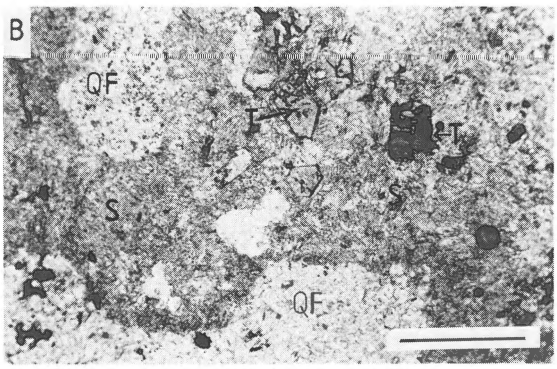
B
QF
S
QF

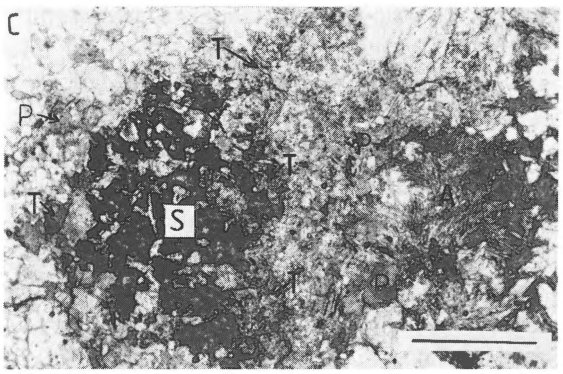
C
P
T
S


D

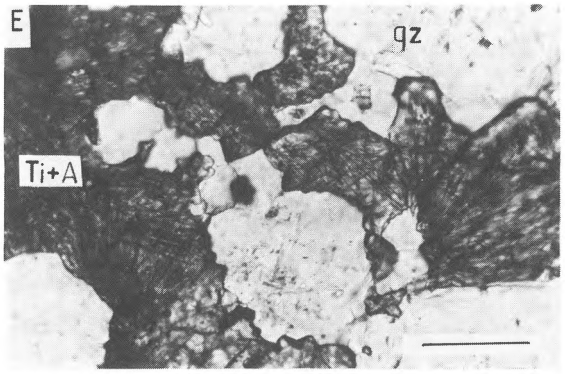
E
qz
Ti+A

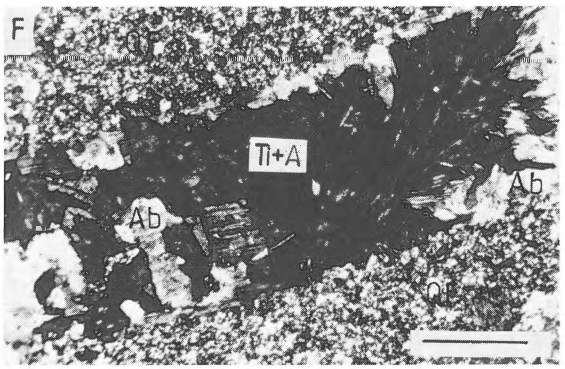
F
Ti+A
Ab
Ab

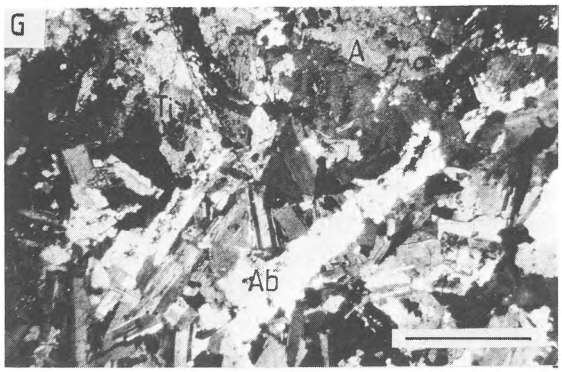
G
A
Ti
Ab

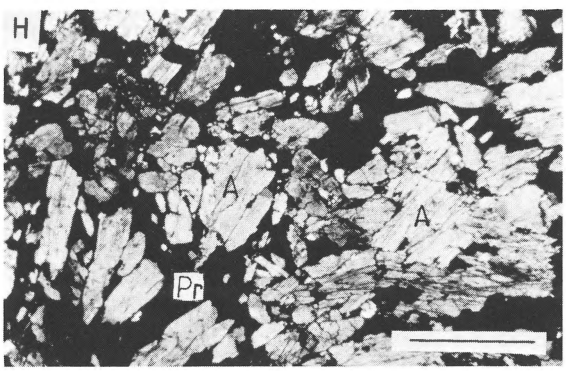
H
A
A
Pr

0.5 m thick. Isoclinal folding within the thicker amphibole matrix demonstrates the pre-deformational age of the brecciation.

In thin section amphibole is seen to form the matrix to the breccia, as well as forming radial growths penetrating the fabric of the felsic metavolcanic breccia fragments and wall rocks. The amphibole filling the matrix comprises large, light green, parallel orientated grains, while the amphiboles penetrating the felsic volcanics are small colourless needles. Amphibole growth clearly postdates phlogopite formation, nucleating around phlogopite grains, and in the sericite aggregates (eg Fig. 2c), as well as forming unoriented rosettes of acicular amphibole in the host volcanics. Amphibole growth probably started in the felsic volcanics prior to the fracturing and brecciation, as part of the contiuous process of alteration during the development of the mafic breccia dyke. After the brecciation amphibole growth continued, occurring chiefly in the intersticies between the fragments. Sphene forms large (up to 5 mm) hydrothermally developed blasts in the felsic metavolcanite. Intergrowths of acicular sphene and amphibole (Fig. 2e) show that sphene development is related to the amphibole stage of alteration. The replacement of relict magmatic feldspar in the felsic metavolcanite by sphene-amphibole intergrowths (Fig. 2f) testifies to the high mobility of Ti during the alteration process. Scapolite is also developed in the breccia matrix. An apparent variation in amphibole composition along the length of the breccia is indicated by the amphibole in the northern part of the breccia having a much lighter colour than that in the south.

The mafic intrusive

The mafic intrusive thought to be genetically related to the brecciation process is exposed at the southern, more mafic end of the breccia. The mafic intrusive is a coarse-grained, hornblende-feldspar rock with minor amounts of interstitial sulphides. Irregular fragments of felsic metavolcanic have been caught up and partially assimilated into the mafic magma, producing clots of hybrid, intermediate material. This rock differs from the usual type of metagabbro seen in Bergslagen, with its apparently more mafic character and abundant macroscopically visible sulphides. Spatial relationships suggest the mafic intrusive underlies the long, narrow breccia dyke.

In thin section the mafic rock shows a relict magmatic texture with intergrowths of large greenish amphibole and subhedral feldspar (Fig. 2g). The feldspar is partially replaced by amphibole and sphene. There is no textural evidence to indicate the magmatic precursor to the amphibole. The green amphibole shows patchy alteration to a colourless amphibole. Some green biotite is also present. Sphene poikiloblasts up to 3 mm are present together with 1 mm grains of pyrrhotite, chalcopyrite and magnetite.

The Ni-Cu-Fe marginal skarn

The skarn mineralization, located on the NE part of the breccia zone (Location 914, Fig. 1) comprises aggregates of massive Ni-bearing pyrrhotite with lesser amounts of chalcopyrite and pyrite. Fragments of felsic metavolcanic in and adjacent to the skarn show the same skarn alteration as seen in the rest of the breccia dyke. A petrographic investigation by Zakrzewski (1988) also demonstrated the presence of pentlandite, mackinawite, marcasite and rare grains of molybdenite, this last probably being related to the nearby younger phase of W-Mo mineralization (e.g. Baker & Hellingwerf, in press). The less massive parts of the skarn comprise intergrowths of idiomorphic dark amphibole and interstitial sulphides.

In thin section the amphibole grains are separat-

←

Fig. 2. (a) Spotted appearance of altered metavolcanic due to phyllosilicate growth (Hammer head approx. 10 cm); (b) Sericitic alteration with tourmaline grains developing (sample 913). bar = 1 mm; (c) Concentric growths of tourmaline and phlogopite around very fine grained sericitic aggregates (sample 916). bar = 1 mm; (d) Coarse amphibole breccia with angular fragments of volcanite up to 25 cm; (e) Accicular intergrowths of sphene and amphibole (sample 930). bar = 0.25 mm; (f) Sphene – amphibole intergrowths replacing relict magmatic feldspar (sample 918). bar = 0.5 mm; (g) Amphibole and relict magmatic feldspar in mafic intrusive (sample 927). bar = 1 mm; (h) Amphibole grains separated by a matrix of pyrrhotite (sample 914). bar = 1 mm; T, tourmaline; QF, quartz-feldspar matrix; S, sericite; P, phlogopite; A, amphibole; Ti, sphene; Pr, pyrrhotite; Ab, albite.

ed by a matrix of pyrrhotite (Fig. 2h), the interstitial pyrrhotite producing a texture similar to that seen in the mafic instrusive. The amphibole grains are cracked, with pyrrhotite filling the fractures.

Mineral chemistry

Representative microprobe analyses of mineral phases from Annehill breccia dyke and related rocks are contained in Table 1. Analyses were made using a Cambridge Instruments GEOSCAN, using an on line ZAF correction procedure. Petrographic observations given above show that tourmaline, micas and amphibole are related to the initial, pre-brecciation, pervasive alteration, while amphibole and sphene growth are related to the later phase of brecciation.

Tourmaline

The tourmalines analysed in three samples are dravites, with MgO/FeO <2. F contents vary from 0.17 to 0.40, while Cl was below detection limit. In terms of the classification of Slack (1982), the MgO/FeO ratios of the Annehill tourmalines are compatible with a hydrothermal origin.

Tourmaline is generally associated with granitic systems or massive sulphides, and is less commonly related to mafic magmatism. Appel (1984, 1985) documents tourmaline related to layered mafic intrusives and exhalative scheelite mineralization from Isua, Greenland. The field of average Isua tourmalines is shown together with the Annehill tourmaline in a $100 \times FeO/(FeO + MgO)$ versus $100 \times Na_2O/(Na_2O + CaO)$ plot (Fig. 3). Also shown are the fields of tourmalines from Hjulsjö, Bergslagen (Baker & De Groot, 1983), Umbertana, Australia (Lottermoser & Plimer, 1987), and Nora-Viker, Bergslagen (Hellingwerf et al., 1988). The Annehill tourmalines do not coincide with the Isua samples, which in terms of Fe and Mg form a field intermediate between the more iron rich Nora-Viker tourmalines from a sedimentary-exhalative Zn mineralization, and the Mg rich tourmalines from a Mg-rich zone developed by sub-seafloor hydrothermal in the felsic metavolcanics at Hjulsjö. The Annehill tourmalines have higher

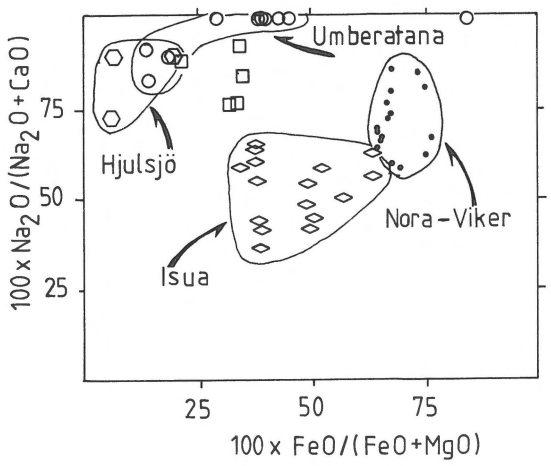

Fig. 3. Tourmaline analyses from Annehill, plotted as open squares, in terms of $100 \times Na_2O/(Na_2O + CaO)$ v $100 \times FeO/(FeO + MgO)$ with fields of tourmaline from Hjulsjö (Baker & De Groot, 1983), Isua (Appel, 1984, 1985), Umberatana (Lottermoser & Plimer, 1987), and Nora-Viker (Hellingwerf et al., 1988).

$Na_2O/(Na_2O + CaO)$ ratios than the Isua samples, and in this respect are closer in composition to tourmalines from a granitic system at Umberatana (Lottermoser & Plimer, 1987).

Micas

The oldest alteration phase seen in thin section is the development of sericitic aggregates in the felsic metavolcanics. Analysis shows that with a K_2O content too low for ordinary muscovite, this is probably hydromuscovite (Table 1). Phlogopite (Mg:Fe>2:1) is present in the aggregates with tourmaline. While Cl contents are low, F varies up to 2 wt%, and shows a positive correlation with Mg and Ti, and negative correlation with Al and K (Fig. 4), though there are insufficient analyses to statistically confirm this tendency. The hydromuscovite analyses, with lower F contents than the phlogopite, tend to follow the phlogopite correlations. Also shown in Figure 4 are the Annehill tourmalines which show a possible weak negative trend between F and Al and Ti.

Amphiboles

The amphiboles of the initial pre-brecciation alteration, later brecciation, and mafic intrusive are all

Table 1. Representative microprobe analyses of minerals from Annehill.

Samples	Amphiboles					
	AI	ABA	ABB	ABC	ABE	ABF
SiO_2	55.51	54.60	58.60	56.81	43.83	43.06
TiO_2	0.08	0.04	0.04	0.02	0.79	0.79
Al_2O_3	0.38	0.51	1.97	0.56	7.95	9.21
FeO	10.47	5.18	4.65	4.13	21.38	22.20
MnO	0.01	0.01	0.01	0.01	0.15	0.19
MgO	17.88	20.74	19.97	21.55	8.79	7.98
CaO	11.08	11.94	10.67	12.30	11.30	11.39
Na_2O	1.18	0.36	1.37	0.37	1.54	1.90
K_2O	0.06	0.05	0.06	0.01	0.70	0.88
Cl	0.01	0.00	0.01	0.00	0.33	0.37
Total	96.66	93.43	97.35	95.76	96.94	97.97

Samples	Phlogopite			Hydromuscovite	
	BIA	BIB	BID	PRA	PRB
SiO_2	38.06	36.65	41.24	41.33	43.33
TiO_2	0.54	0.35	1.02	0.06	0.04
Al_2O_3	17.83	19.08	11.72	29.68	34.67
FeO	9.65	9.62	7.76	3.04	1.93
MnO	0.03	0.01	0.03	0.01	0.00
MgO	17.90	17.38	22.10	4.04	2.31
Na_2O	0.24	0.18	0.13	0.05	0.08
K_2O	10.25	10.08	8.64	7.57	7.68
Cl	0.02	0.02	0.03	–	–
F	1.08	1.03	1.99	0.53	0.12
Total	95.60	94.40	94.66	86.77	90.88

Samples	Tourmalines				
	TOA	TOB	TOG	TOD	TOE
SiO_2	35.95	35.66	36.31	35.70	35.81
TiO_2	0.21	0.21	0.08	0.35	0.15
Al_2O_3	31.64	31.53	34.12	32.37	31.99
FeO	4.15	4.48	2.58	4.57	4.65
MnO	0.00	0.01	0.01	0.01	0.01
MgO	8.71	8.86	9.47	8.49	8.98
Na_2O	2.47	2.59	2.56	2.81	3.06
CaO	0.78	0.79	0.35	0.54	0.25
F	0.37	0.23	0.21	0.17	0.40
Total	84.28	84.36	85.69	85.01	85.30

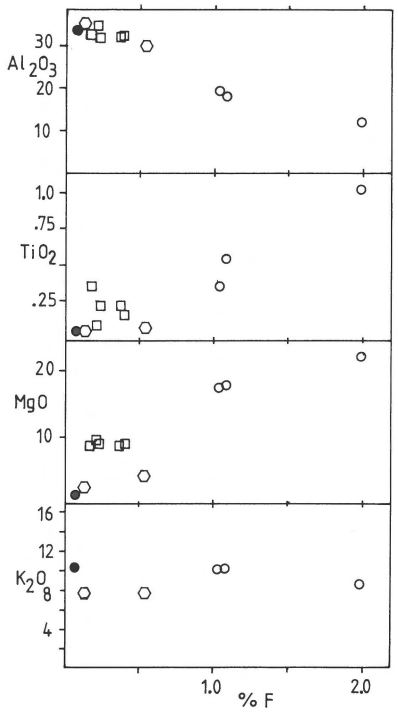

Fig. 4. Oxide variations versus %F content of phyllosilicates and tourmaline from Annehill. Open circles – phlogopite; filled circles – sericite; hexagon – hydromuscovite; square tourmaline.

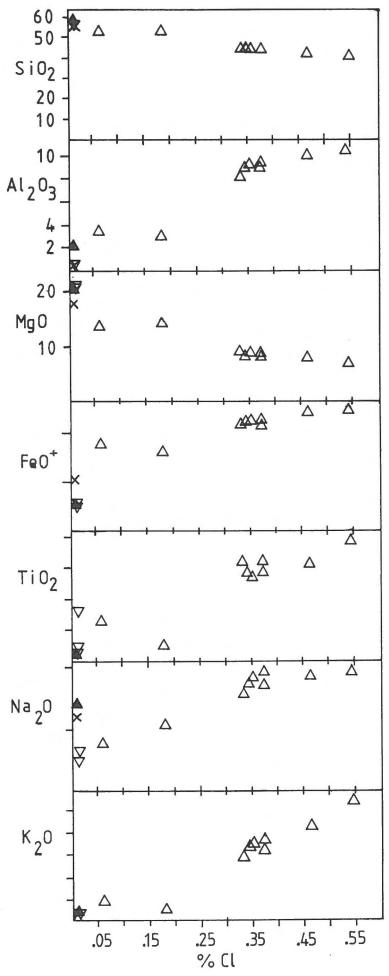

Fig. 5. Oxide variations versus % Cl in amphiboles from Annehill. Symbols refer to amphibole analyses from different samples.

Ca amphiboles, either with low Al_2O_3 (up to 4 wt%) or high Al_2O_3 (8-12 wt%) varying from tremolite to hornblendes. While the micas show a correlation between F and some major elements, the amphiboles show similar positive correlations between Cl and Al, total Fe, Ti, Na and K, and negative correlations with Si and Mg (Fig. 5). Weak negative correlations are present between F and Fe, Ti and Na. The highest Cl values are present in amphiboles from the mafic intrusive. The correlation between Cl and other elements is a strong argument for the hydrothermal nature of the amphiboles in the Annehill breccia and related rocks.

The paragenetic sequence of formation of these hydrothermal minerals taken together with the mineral chemistry suggests the influx and mobility of elements as shown in Fig. 6. The participation of volatiles in the alteration process follows an order of increasing atomic weight from B to F to Cl, corresponding to the development of tourmaline, phlogopite and amphibole. This sequence of volatile involvement is matched by the introduction of K, Mg, Fe, Na and Ca. The continuous nature of the alteration suggests that the entire process is one of skarn formation, not just that part where Ca is introduced into the system.

Geochemical variations

Major elements were analysed using standard XRF techniques, except Ti and Mn, analysed by ICP, along with Be, Li, B, V and Y. All other trace elements by INAA, using the procedures of De

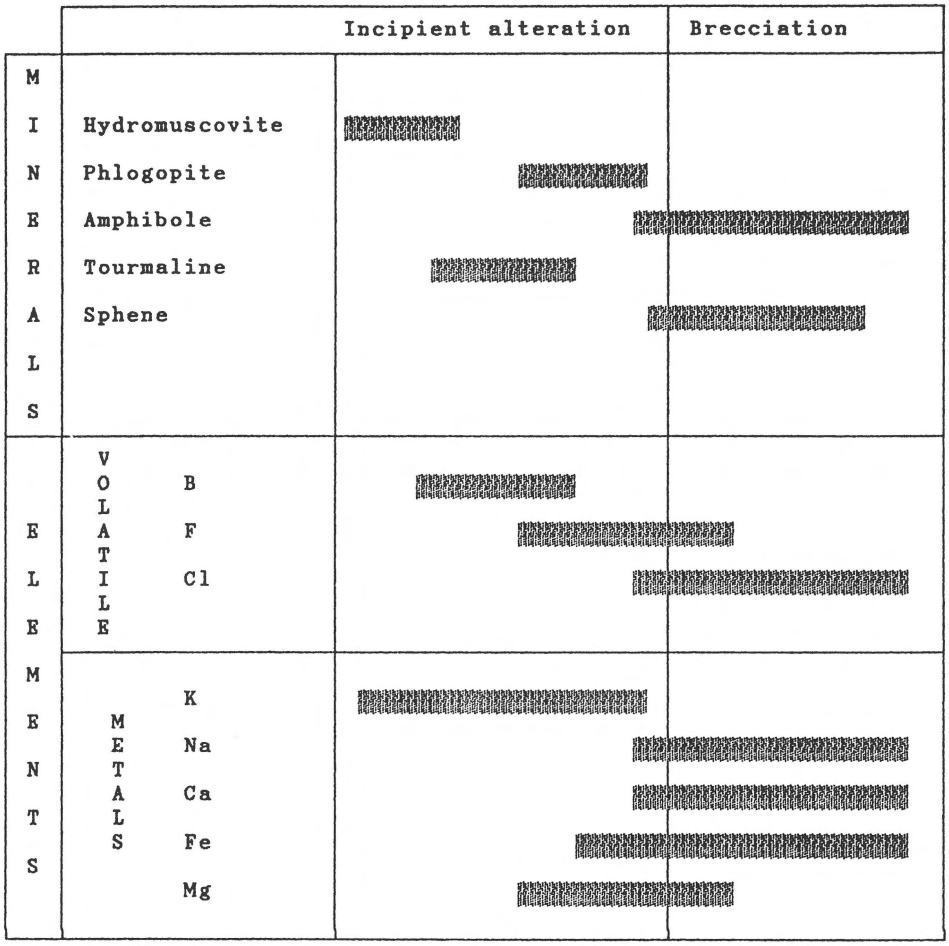

Fig. 6. Paragenetic sequence of hydrothermal minerals from petrographic observations, together with volatile and metal distributions, interpretation based on microprobe data.

Bruin (1983), except Ni, Cu, Zn, Ga, Rb, Sr, Zr, Ba and Pb, analysed by XRF using the method of VieLeSage et al. (1979).

Variations with major elements

Fe tends to increase from the least altered felsic metavolcanic through the pervasively altered metavolcanics and breccia to mafic intrusive, and is a useful indicator of the alteration process. With increasing Fe there is a progressive increase in Ca and Mg, and decrease in Si (Fig. 7). The Na/Al ratio, rather than just Na shows a progressive increase with Fe, reflecting the role of amphibole in the system. The B rich samples have lower Na and higher K than the other pervasively altered material, and coincide with the highest Rb and Li, and lowest Co.

While Mg is often expected to correlate with Ni and other transition elements in magmatic Ni-systems (e.g. Groves et al., 1979), not only is the instrusive responsible for the breccia mafic rather than ultramafic, there is a predominant hydrothermal component in the system. Mg therefore only shows a slight positive correlation with Ca, Co, Pb and Sm, and negative correlation with Zr. Fe rather than Mg correlates with the transition elements Ti, Mn, Co and V, and Fe also shows positive correlations with Be, Pb, Sc and Eu.

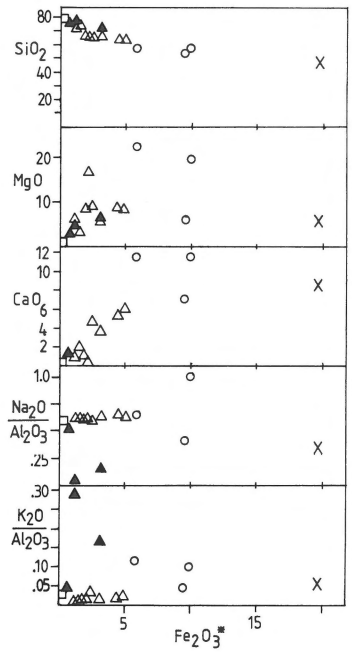

Fig. 7. Major element variations in samples from Annehill. Square-least altered felsic metavolcanite; triangle – pervasively altered, filled triangle – with high B content; circle – breccia; cross – mafic intrusion.

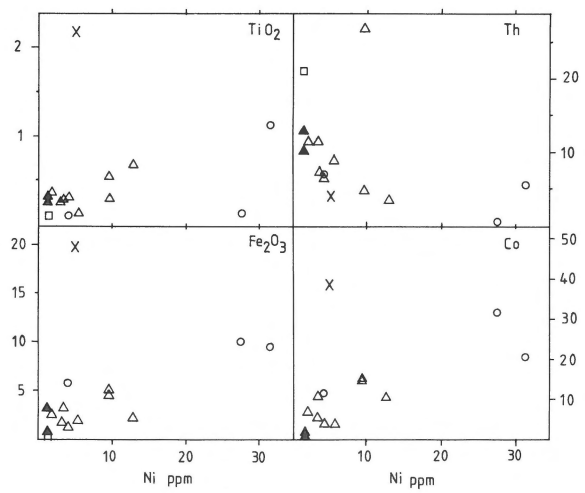

Fig. 8. Variation of Ni with TiO_2, Fe_2O_3, Co and Th; symbols as in Fig. 7.

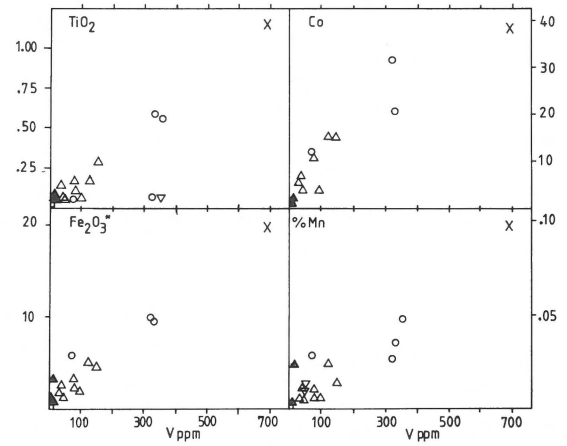

Fig. 9. Variation of V with Ti, Fe, Co and Mn; symbols as in Fig. 7.

Transition elements

The transition elements show good interelement correlations. There is an increase from least altered metavolcanic through breccia to mafic rock for V, Ti, Co and Mn. Ni is low in the mafic rock, but shows a positive correlation for Fe, Ti and Co and a negative trend with Th in the breccia (Fig. 8). V shows much better correlations (Fig. 9), positive with Ni, Ti, Fe, Mn, Co, Mg, Na, K, Sr, Be and Li, and negative with Cr, Rb and B.

The three pyrrhotite-bearing samples from the sharn ores contain both V and Ni up to 700 ppm. Ni shows an apparent positive correlation with W, P and Tb, and negative with Se, Sc, Cu, Zn and Ce/Tb (Fig. 10). The Cu content varies from 219 to 959 ppm.

Se content varies from 8 to 26 ppm in the ore samples. The S/Se ratio has been used by some authors to discriminate between magmatic, volcano-sedimentary sulphides, which have progressively higher S/Se ratios (e.g. Groves et al., 1979; Naldrett 1981). S has not been measured in these samples, but by assuming that all Fe is combined in pyrrhotite, the S content can be estimated, giving S/Se ratios of about 29000, 3800 and 6000. The same samples have Ni/Cu ratios of .04, .93 and 4.3. The highest S/Se, corresponding with the lowest Ni/Cu ratios come from the sample closest to the breccia, and is higher than is usually found in magmatic systems.

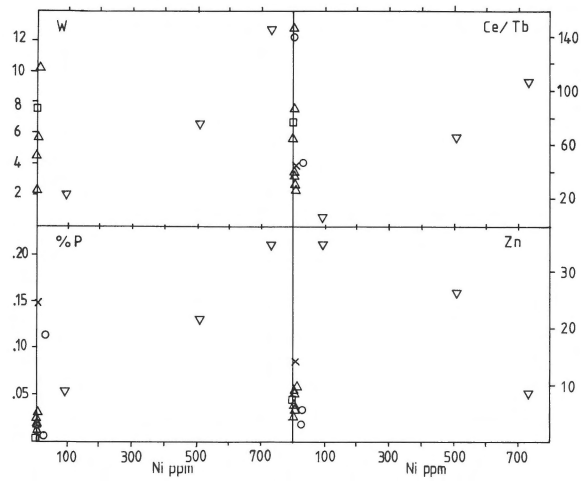

Fig. 10. Variation of Ni with W, P, Zn and Ce/Tb in pyrrhotite ore samples (inverted triangle, other symbols as in Fig. 7).

Rare earth elements

REE patterns of Annehill samples are shown in Fig. 11. The least altered felsic metavolcanic shows a concave pattern with small negative Eu anomally, while the mafic intrusive has a fractionated pattern from La to Lu. This pattern is similar to that of the first generation of mafic sills in Bergslagen (Baker, unpubl. data). The pervasively altered samples show a wide variation in light and middle REE, converging towards the heavy REE. The highest and lowest Light REE are from the high B samples. The remaining pervasively altered samples form a tighter envelope which is roughly bounded at the lower side by the least altered metavolcanic and at the upper side by the mafic intrusive. This suggests that the REE patterns in the pervasively altered rocks result from a successive addition of material with an REE pattern comparable to the mafic rock to one similar to the least altered metavolcanic. The brecciated samples are similar to the pervasively altered samples, as regards REE. Two of the pyrrhotite ore samples show heavy REE enrichments, while the third is similar to the pervasively altered rock.

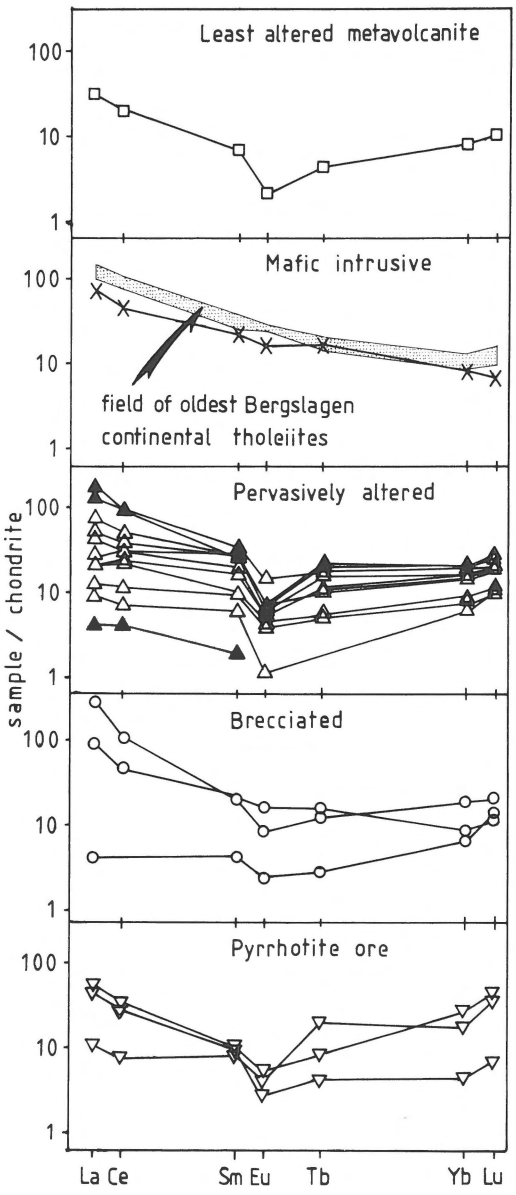

Fig. 11. Chondrite normalized REE patterns (using chondrite values of Evanson et al., 1979) for samples from Annehill.

Genesis of the Annehill mafic breccia dyke

A two stage model is proposed for the hydrothermal alteration and development of the mafic breccia dyke and related Ni-Cu-Fe mineralization. Emplacement of the mafic magma, along a pre-existing zone of weakness, initiated a hydrothermal cell in the upper crust (Fig. 12a). Mafic magmas are generally not enriched in volatiles, so the B, F and Cl participating in the development of sericite, tourmaline and phlogopite, and the first growth of

amphibole, were probably derived from the felsic metavolcanic wall rocks. These volcanics were deposited in a submarine environment (e.g. Oen et al., 1982; Oen, 1987), and are likely to have gained high volatile contents during sub-seafloor alteration processes (e.g. Baker & De Groot, 1983). While metals have clearly been derived from the tholeiitic intrusive, there will only have been a minor fluid contribution from the magma, perhaps leaked along fault structures during emplacement. Clearly defined alteration zones have not been identified at Annehill, where the narrow width of the breccia zone and the lack of detailed drill core data precludes this kind of interpretation. While the hydrothermal minerals described above were developing in the felsic metavolcanics, the separation of Ni, S and other elements into a hydrothermal phase, and the auto-metamorphism of the crystallizing mafic rock was taking place. The entrapment of Ni in this fluid explains the low Ni-content of the mafic intrusive. Brecciation of the partially altered felsic volcanic could have been triggered by fault movements and/or pressure build up in the crystallizing magma. Pressure release through brecciation allowed injection of the Ni-bearing hydrothermal fluids into the host to form the skarn mineralization, and at the same time the amphibole rich mafic matrix to the breccia (Fig. 12b). The Annehill Ni-mineralization is concentrated chiefly along the margin of the breccia dyke, due to enhanced permeability (Sillitoe, 1985). Metal transport probably also occurred by Cl complexing, indicated by the Cl – major element correlations seen in amphiboles, and by the complete (auto) alteration of the mafic rock to an amphibole – feldspar rock.

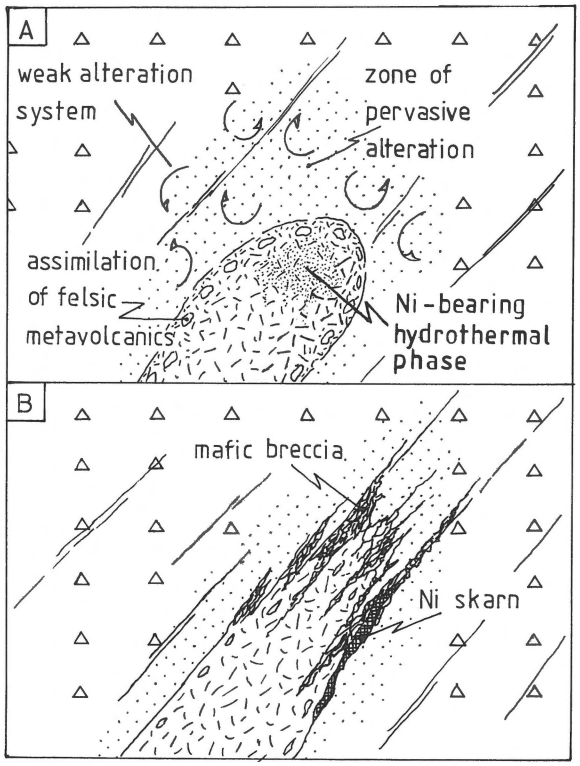

Fig. 12. Sketch showing proposed evolution of the Annehill mafic breccia and Ni-Cu-Fe mineralization (see text for explanation).

Breccias and Ni-mineralization

While breccia-related mineralization is fairly common (e.g. Sillitoe, 1985), there are few reports of mineralizations related to mafic breccias. Magmatic-hydrothermal breccias are generally related to intrusives of felsic to intermediate composition (Sillitoe, 1985), in which tourmaline is a common accessory. Tourmalinization and other wall rock alteration around a breccia pipe at Ilkwang, Korea, related to pyrrhotite-chalcopyrite mineralization has been described by Fletcher (1977). Sericitization characterizes the breccia pipe, and propylitic alteration the wall rocks, with epidote, chlorite, tremolite and calcite, while tourmaline and garnet are developed across the contact between the breccia and host rock. The tourmaline-bearing, Proterozoic Cu-Mo mineralized Tribag breccia pipes of Ontario, Canada, are associated with continental rifting, their position determined by pre-existing fault patterns (Norman & Sawkins, 1985).

Ni-mineralizations related to breccias are uncommon, and where found are generally considered to be remobilized, postdating magmatic ore formation (e.g. Groves et al., 1979). A possible exception to this may be Windarra, Australia (Lusk, 1976). Reported Swedish breccia-related mineralizations tend to be intramagmatic, such as the komataiitic breccia at Knafke, N. Sweden

(Nilsson, 1985). The pyrrhotite-pentlandite-chalcopyrite mineralization at Skjaekerdalen, Norway comprises seven separate sulphide mineralizations related to a 4 × 1.5 km intrusive gabbro and breccia containing fragments of magmatic and host rock (Boyd & Nixon, 1985). A magmatic origin of the Ni ore is proposed, remobilized by later tectonic processes. One of the largest breccia-related Ni-mineralizations is Pechenga-Vazuga, Kola peninsula, USSR (Glaskovsky et al., 1977; Gorbunov et al., 1985). The mineralization, located in a NW trending graben evolved during an intracratonic volcano-tectonic Svecokarelian event (Gorbunov et al., 1985), contains some of its highest grade mineralization in breccia ores. The breccias comprise fragments of mafic magmatic rock, talcose phyllites and tuffs cemented by a sulphide matrix. Veinlets of pure sulphides in the host rock to the breccia are taken as evidence of forcible injection of a sulphide magma. The breccia ores can always be traced a short distance back into the adjacent magmatic rock, supporting a magmatic origin for the ore. Ni/Cu ratios increase from mineralization in the mafic host out into the breccia. Minor chlorite, calcite and quartz in the matrix are evidence of a hydrothermal component in the formation of the breccia.

Hydrothermal processes and Ni-mineralizations

Discussions on the origins of Ni ores emphasize their magmatic nature (e.g. Groves et al., 1979; Naldrett, 1981). Nevertheless late stage or post magmatic hydrothermal activity is documented in a number of cases. Lusk (1976) argued for a volcano-sedimentary exhalative origin for some Ni-mineralizations. Windarra, with a stratigraphic control on lenticular Ni-S mineralization, a spatial association with Fe ores and discontinuous metasediment layers in metatuffites, and a lack of wall rock alteration is the best known example (e.g. Lusk, 1976; Groves et al., 1979), implying a high element mobility. Mostly, however, a post magmatic redistribution is invoked. Talkington & Watkinson (1984) suggest redistribution of Cu-Ni-S occurs during late stage deuteric autometasomatism. The presence of chlorite and amphibole in the mafic host to the mineralization at Koillismaa, Finland testifies to the role of transport and deposition of sulphides, and is also considered important for concentration of PGE (Piispanen & Tarkian, 1984).

The roles of B, F and Cl in the alteration and brecciation process at Annehill, together with the alteration of a primary mineral association to amphibole and mica in the mafic rock testifies to the important role of volatile complexing and element transport in this mineralization.

Conclusions

The Annehill breccia dyke is an unusual Proterozoic Ni-mineralization in which hydrothermal processes and the involvement of B, F, and Cl have played a major role. The geological and petrological observations, and interpretation of rock and mineral geochemistry given above suggest a two stage model for the development of the breccia dyke and Ni-mineralization. The intrusion of an Fe-tholeiite, post-dating the felsic volcanic rocks, initiated a hydrothermal cell around and above the intrusive. This produced a pervasive alteration of the wall rocks, remobilizing volatiles derived primarily from the felsic volcanics, as well as any hydrothermal fluid expelled from the magma. Metals and other elements were derived from the tholeiite. Alteration phases formed in sequence are hydromuscovite, tourmaline, phlogopite and Ca-amphibole, corresponding to B, F and Cl metasomatism and the input of K, Mg, Na, Ca and Fe. The development and concentration of the Ni-bearing hydrothermal fluid within the crystallizing mafic rock also occurred at this time, creating a pressure build up. The main phase of brecciation released Ni and other elements in a hydrothermal phase to form both the matrix to the breccia and the marginal Ni skarn mineralization.

Acknowledgements

This paper has benefited from the critical comments of I.S. Oen, Terry Finlow-Bates, Ian Plimer

Table 2. Analyses of samples from Annehill; 912 – least altered felsic metavolcanic; 910, 911, 917, 929 – brecciated samples; 914, 923, 924 – pyrrhotite bearing samples; 927 – mafic intrusive; – all others, pervasively altered. Major elements by XRF except Mn and Ti by ICP. Trace elements by INAA, except Be, B, Li, V, Y, by ICP, and Ni, Cu, Zn, Ga, Rb, Sr, Zr, Pb by XRF. All elements in 911 by ICP, and major elements in 914, 923, 924 by ICP.

Sample (wt. %)	910	911	912	913	914	916	917	918	919	920
SiO_2	53.24	–	79.30	73.92	–	63.62	56.74	70.31	62.36	70.92
TiO_2	0.97	0.92	0.03	0.05	0.10	0.07	0.08	0.05	0.45	0.12
Al_2O_3	15.27	14.85	11.32	13.17	1.98	12.25	1.35	12.86	11.24	12.84
Fe_2O_3	9.48	8.65	0.28	0.68	50.04	2.46	5.80	1.12	4.46	3.11
MnO	0.05	0.06	0.00	0.03	0.05	0.01	0.04	0.00	0.02	0.00
MgO	5.96	6.45	0.74	2.51	5.34	8.42	22.09	5.75	8.18	5.70
CaO	7.04	7.49	0.01	1.04	4.48	4.51	11.48	0.62	5.09	–
Na_2O	6.31	4.72	6.64	6.68	0.62	7.04	0.87	7.70	7.08	1.63
K_2O	0.68	1.70	0.29	0.48	0.14	0.30	0.16	0.05	0.08	2.04
P_2O_5	0.27	0.26	0.01	0.02	0.12	0.03	0.02	0.06	0.01	0.03
Total	99.25	–	98.61	98.58	–	98.70	98.62	98.52	98.95	96.39
(ppm)										
Be	2.0	7.0	–	3.0	87.0	3.0	6.0	1.0	5.0	1.0
Li	8.0	20.0	4.0	6.0	5.0	5.0	6.0	5.0	3.0	25.0
B	3.0	22.0	2.0	33.0	–	5.0	4.0	2.0	3.0	57.0
V	331.0	357.0	4.0	16.0	343.0	40.0	71.0	46.0	149.0	14.0
Sc	44.57	–	1.60	5.88	44.16	11.14	4.47	6.33	8.70	6.56
Cr	35.62	–	63.05	40.66	130.00	–	–	23.00	21.94	33.40
Co	20.43	23.0	–	1.35	146.89	6.13	11.39	3.09	14.40	0.18
Ni	31.50	28.0	1.29	1.25	82.50	1.82	4.03	3.98	9.47	1.26
Cu	–	2.0	1.2	–	1090.0	1.5	–	–	–	–
Zn	5.53	21.0	7.18	6.88	34.60	8.17	9.35	7.92	5.01	4.08
Ga	14.90	–	9.75	9.28	30.90	18.00	2.86	9.67	12.00	11.40
As	2.79	–	–	21.07	–	–	0.73	–	–	2.56
Se	–	–	–	–	6.99	–	–	–	–	–
Rb	32.20	–	23.00	38.50	–	18.00	15.70	9.88	8.52	45.50
Sr	88.00	181.0	2.37	11.10	9.92	1.89	–	5.33	–	–
Y	21.0	22.0	7.0	5.0	24.0	18.0	41.0	8.0	41.0	11.0
Zr	95.40	–	121.00	242.00	104.00	216.00	36.70	206.00	138.00	219.00
Nb	6.74	–	14.80	12.50	3.33	13.50	5.00	8.33	22.40	11.10
Sb	–	–	–	1.59	–	–	0.36	–	–	1.18
Cs	6.51	–	0.87	2.32	4.70	3.41	1.90	0.49	–	1.87
Ba	62.9	90.0	53.7	35.2	–	75.1	62.8	60.9	89.4	102.0
La	33.00	37.0	11.10	1.54	3.90	64.00	105.00	4.63	9.54	47.70
Ce	44.29	110.0	19.29	3.94	7.17	84.53	104.00	11.10	29.93	90.20
Sm	4.88	–	1.56	0.44	1.85	5.97	4.54	2.12	6.78	7.74
Eu	1.43	–	0.18	–	0.36	0.60	0.75	0.33	0.60	1.24
Tb	0.95	–	0.25	–	1.14	0.58	0.74	0.29	1.16	1.05
Yb	2.30	–	1.97	1.88	4.35	3.49	5.01	1.82	4.98	4.65
Lu	0.46	–	0.38	0.40	1.34	0.69	0.85	0.35	0.91	0.76
Hf	2.20	–	4.31	6.61	0.74	5.86	0.88	5.80	4.87	5.74
Ta	–	–	1.04	0.75	–	–	–	0.63	1.61	0.63
W	–	6.0	7.6	4.4	2.0	5.6	–	–	–	2.3
Pb	4.61	15.0	6.51	3.42	–	6.06	9.56	5.14	9.27	7.96
Th	5.47	–	21.09	9.88	–	11.11	6.90	6.31	26.58	12.60
U	–	–	–	–	–	–	–	–	2.32	1.59

Table 2. (Continued).

Sample (wt.%)	921	922	923	924	925	926	927	928	929	930
SiO_2	64.11	64.52	–	–	75.95	65.19	46.43	72.17	56.74	61.72
TiO_2	0.15	0.25	–	–	0.08	0.07	1.90	0.20	0.10	0.25
Al_2O_3	8.89	14.16	–	–	12.19	14.00	11.82	12.85	0.86	11.08
Fe_2O_3	2.11	3.12	19.02	21.02	1.11	1.85	19.74	1.53	9.92	4.97
MnO	0.01	0.01	0.02	0.01	0.00	0.01	0.13	0.01	0.03	0.03
MgO	16.15	5.10	0.70	0.20	4.20	7.90	5.72	2.83	19.56	7.70
CaO	0.14	3.47	4.97	0.73	–	1.00	8.58	1.78	11.46	5.89
Na_2O	5.31	8.65	0.02	0.01	0.33	8.23	4.07	7.79	0.86	6.85
K_2O	0.06	0.06	–	–	3.47	0.08	0.66	0.05	0.08	0.15
P_2O_5	0.01	0.02	0.30	0.48	0.02	0.03	0.33	0.05	0.01	0.01
Total	96.95	99.36	–	–	97.36	98.35	99.37	99.25	99.63	98.65
(ppm)										
Be	2.0	4.0	1.0	–	2.0	3.0	5.0	2.0	11.0	5.0
Li	10.0	3.0	16.0	2.0	24.0	6.0	6.0	2.0	4.0	5.0
B	1.0	3.0	1.0	1.0	28.0	–	1.0	2.0	2.0	5.0
V	79.0	77.0	42.0	39.0	6.0	96.0	691.0	31.0	322.0	123.0
Sc	7.70	7.21	0.98	0.31	6.97	5.08	48.78	6.14	25.19	26.70
Cr	15.89	10.57	110.90	214.90	45.80	12.63	12.43	35.21	14.87	83.88
Co	9.94	9.92	368.90	304.00	0.46	3.03	38.34	4.55	31.30	14.58
Ni	12.80	3.45	499.00	723.00	–	5.32	4.94	3.19	27.50	9.48
Cu	–	–	5500.0	268.0	–	–	34.1	–	–	–
Zn	9.26	8.89	26.20	8.50	5.46	6.02	14.10	6.43	2.90	7.82
Ga	11.70	16.10	7.26	9.42	15.80	16.30	21.30	9.75	–	14.80
As	–	2.18	4.64	16.76	–	–	1.63	1.43	–	2.35
Se	–	–	20.20	14.70	–	–	–	–	–	–
Rb	10.10	8.68	–	–	94.20	11.90	5.48	8.95	5.14	14.20
Sr	1.51	1.44	8.86	4.42	1.46	13.70	27.40	–	–	2.81
Y	5.0	27.0	22.0	16.0	8.0	22.0	24.0	14.0	11.0	37.0
Zr	140.00	242.00	32.10	30.60	141.00	229.00	98.50	219.00	30.20	189.00
Nb	16.40	14.50	3.26	2.25	17.80	3.94	7.36	13.20	3.56	11.60
Sb	–	–	0.88	0.95	–	–	–	0.21	–	–
Cs	0.74	–	–	–	5.29	0.44	–	–	–	–
Ba	72.8	38.0	–	–	112.0	93.2	–	66.4	51.3	134.0
La	3.34	7.68	20.25	16.00	26.81	15.70	26.45	7.97	1.53	18.79
Ce	6.85	22.68	32.34	26.60	48.17	28.90	44.42	20.59	–	37.27
Sm	1.34	3.76	2.38	2.16	6.28	4.48	5.20	2.32	1.00	6.05
Eu	0.10	0.48	0.45	0.24	0.54	0.46	1.41	0.39	0.21	0.64
Tb	–	0.63	0.49	0.25	0.90	0.67	1.00	0.32	0.17	1.27
Yb	1.44	3.60	6.54	1.09	3.83	3.98	2.04	2.18	1.71	4.95
Lu	0.39	0.66	1.64	0.26	0.70	0.73	0.25	0.42	0.56	1.02
Hf	4.17	6.58	–	–	5.11	5.92	1.52	5.95	0.52	4.99
Ta	1.38	0.75	–	–	1.29	–	–	0.71	–	–
W	10.1	–	6.6	12.7	3.9	–	–	4.4	–	–
Pb	5.28	6.54	15.20	12.10	6.53	5.74	–	4.79	7.27	10.70
Th	3.20	6.81	–	–	10.70	8.60	4.05	11.13	0.42	4.48
U	–	1.81	1.75	–	4.26	–	–	–	–	–

and Marek Zakrzewski. Neutron activiation analyses were made at the IRI, Technical University of Delft, and the assistance of M. de Bruin and coworkers is gratefully acknowledged. XRF major and trace element analyses were provided by F.F. Beunk. ICP analyses were made by G. Patsauer at LKAB's Stockholm laboratory. Microprobe facilities were provided by the WACOM, a working group for analytical geochemistry subsidized by the Netherlands Organization for the Advancement of Pure Research (ZWO).

References

Appel, P.W.U. 1984 Tourmaline in the early Archaean Isua supracrustal belt, West Greenland – J. Geol. 92: 599–605

Appel, P.W.U. 1985 Stratabound tourmaline in the Malene supracrustals, West Greenland – Can. J. Earth Sci. 22: 1485–1491

Baker, J.H. & De Groot, P.A. 1983 Proterozoic seawater – felsic volcanics interaction, W. Bergslagen, Sweden. Evidence for high REE mobility and implications for 1.8 Ga seawater compositions – Contrib. Mineral. Petrol. 82: 119–130

Baker, J.H. & Hellingwerf, R.H. in press.The geochemistry of tungsten – molybdenum bearing granites and skarns from West Bergslagen, Central Sweden. (IAGOD, Luleå) – E. Schweizerbart'sche Verlagsbuchhandlung, Stuttgart 5: 2

Blomberg, A. 1879 Beskrifning til kartbladet Hjulsjö – Sver. Geol. Unders. Ser Aa 69: 40 pp

Boyd, R. & Nixon, F. 1985 Norwegian nickel deposits: a review. – Geol. Surv. Finland Bull. 333: 363–394

De Bruin, M. 1983 Instrumental neutron activation analysis – a routine method – PhD thesis, Delftse Univ. Pers, 270 pp

Evenson, N.H., Hamilton, P.J. & O'Nions, R.K. 1978 Rare earth abundances in chondritic meteorites – Geochim. Cosmochim. Acta 42: 1199–1212

Fletcher, C.J.N. 1977 The geology, mineralization and alteration of Ilkwang Mine, Republic of Korea. A Cu-W-bearing tourmaline breccia pipe – Econ. Geol. 72: 753–768

Geijer, P. & Magnusson, N.H. 1944 De Mellansvenska järnmalmernas geologi – Sver. Geol. Unders. Ser Ca 35: 654 pp

Glaskovsky, A.A., Gorbunov, G.I. & Sysoev, F.A. 1977 Deposits of nickel. In: Smirnov, V.I. (ed.): Ore deposits of the USSR, II (English transl. D.A. Brown): 3–79

Gorbunov, G.I., Zagorodny, V.G. & Robana, W.I. 1985 Metallogeny of nickel of the eastern part of the Baltic shield and the epochs of ore formation – Geol. Surv. Finland Bull. 333: 17–122

Groves, D.I., Barrett, F.M. & McQueen, K.G. 1979 The relative roles of magmatic segregation, volcanic exhalation and regional metamorphism in the generation of volcanic-associated nickel ores of western Australia – Can. Miner. 17: 319–336

Hellingwerf, R.H., Lilljequist, R. & Ljung, S. 1988 Stratiform Zn-Pb-Fe-Mn mineralization in the Älvlången – Vikern area, Bergslagen, Sweden. In: Baker, J.H. & Hellingwerf, R.H. (eds.): The Bergslagen Province, Central Sweden – Structure, stratigraphy and ore-forming processes. I.G.C.P. project 247. – Geol. Mijnbouw 67: 313–332 (this issue)

Lottermoser, B.G. & Plimer, I.R. 1987 Chemical variation in tourmaline, Umberatana, South Australia – N. Jb. Miner. Monatsh. 7: 314–326

Lusk, J. 1976 A possible volcanic-exhalative origin for lenticular nickel sulfide doposits of volcanic associations, with special reference to those of western Australia – Can. J. Earth Sci. 13: 451–458

Moorman, A.C., Andriessen, P.A.M., Boelrijk, N.A.I.M., Hebeda, E.K., Oen, I.S., Priem, H.N.A., Verdurmen, E.A.Th., Verschure, R.H. & Wiklander, U. 1982 K-Ar and Rb-Sr mineral ages of skarns and associated metabasites and leptites in the Hjulsjö area of the Bergslagen ore province, Central Sweden – Geol. För. Förh. 104: 1–9

Naldrett, A.J. 1981 Nickel sulfide deposits: classifications, composition and genesis – Econ. Geol., 75th Ann. Vol.: 628–685

Nilsson, G. 1985 Nickel-copper deposites in Sweden – Geol. Surv. Finland Bull. 333: 313–362

Norman, D.I. & Sawkins, F.J. 1985 The Tribag breccia pipes: Precambrian Cu-Mo deposits Batchawana Bay, Ontario – Econ. Geol. 80: 1593–1621

Oen, I.S. 1987 Rift-related igneous activity and metallogenesis in S.W. Bergslagen, Sweden – Precambr. Res. 35: 367–382

Oen, I.S., Helmers, H., Verschure, R.H. & Wiklander, U. 1982 Ore deposition in a Proterozoic incipient rift zone environment: a tentative model for the Filipstad-Grythyttan-Hjulsjö region, Bergslagen, Sweden – Geol. Rundsch. 71: 182–194

Piispanen, R. & Tarkian, M. 1984 Cu-Ni-PGE mineralization at Rometöväs Koillismaa Layered complex, Finland – Mineral. Deposita 19: 105–111

Sillitoe, R.H. 1985 Ore-related breccias in volcanoplutonic arcs –Econ. Geol. 80: 1467–1514

Slack, J.F. 1982 Tourmaline in Appalachian – Caledonian massive sulphide deposits and its exploration significance – Inst. Min. Metall. Trans. 91: B81–B89

Talkington, R.W. & Watkinson, D.H. 1984 Trends in the distribution of the precious metals in the Lac-des-Iles complex, northwestern Ontario – Can. Miner. 29: 125–136

VieLeSage, R., Quisefit, J.P., Dejean de la Batie, R. & Faucherie, J. 1979 Utilisation du rayonnement primaire diffusé par l'échantillon pour une détermination rapide et précise des éléments tracés dans les roches – X-Ray Spectrometry 8(3): 121–128

Zakrzewski, M.A. 1988 Mineral parageneses of the sulfide ore deposits of the Bergslagen metallogenic province: 1. Ni-Cu deposits of southern Sweden. In: Baker, J.H. & Hellingwerf, R.H. (eds.): The Bergslagen Province, Central Sweden – Structure, stratigraphy and ore-forming processes. I.G.C.P. project 247 – Geol. Mijnbouw 67: 357–362 (this issue)